

2021-09-20

Australian Plate Subduction is Responsible for Northward Motion of the IndiaAsia Collision Zone and 1,000km Lateral Migration of the Indian Slab

Parsons, Andrew

<http://hdl.handle.net/10026.1/18119>

10.1029/2021gl094904

Geophysical Research Letters

American Geophysical Union (AGU)

All content in PEARL is protected by copyright law. Author manuscripts are made available in accordance with publisher policies. Please cite only the published version using the details provided on the item record or document. In the absence of an open licence (e.g. Creative Commons), permissions for further reuse of content should be sought from the publisher or author.

Australian plate subduction is responsible for northward motion of the India-Asia collision zone and ~1000 km lateral migration of the Indian slab

Parsons AJ¹, Sigloch K^{1,2}, Hosseini K^{1,3}.

Author affiliations:

1. Dept. Earth Sciences, University of Oxford, Oxford, UK.
2. Université Côte d'Azur, CNRS UMR 7329, Géoazur, Sophia Antipolis, France
3. Alan Turing Institute, London, UK

Key Points

- Subduction of Australian oceanic lithosphere drove northward motion of coupled India-Australia plate since onset of collision at 45-40 Ma
- Buoyant Indian continent stalled subduction of Indian slab whilst Australian slab subduction drove motion of coupled India-Australia plate
- ~1000 km north lateral migration of Indian slab occurred to maintain compatibility with plate kinematics of coupled India-Australia plate

Plain Language Summary

To understand the links between plate tectonics and mantle processes, researchers must determine how tectonic plates have moved with respect to the evolving mantle through geological time. To overcome this problem, recent studies use the locations of subducted slabs in the deep mantle to reconstruct plate motions, based on the hypothesis that slabs sink vertically through the mantle, and therefore mark the surface locations of past subduction zones. Here, we test slab sinking hypotheses, and their use in plate reconstruction modelling, by investigating the sinking kinematics of the subducting Indian and Australian slabs during the India-Asia collision. Our analysis indicates that since onset of collision at ~45-40 Ma, the Indian slab migrated laterally, ~1000 km northwards through the mantle, driven by subduction of the neighbouring Australian slab. We arrive at this new interpretation because we interpret Indian and Australian slab kinematics collectively, and with respect to India-Australia plate motions. Our study shows that the sinking behaviour of one slab can influence that of another slab in the same network. Slab-based plate reconstructions should therefore interpret slabs of the same network collectively, and with respect to plate motions, in order to constrain non-vertical slab motions and avoid potentially significant plate reconstruction errors.

Abstract

Distributions of slabs within Earth's mantle are increasingly used to reconstruct past subduction zones, based on first-order assumptions that slabs sink vertically after slab break-off, and thus delineate paleo-trench locations. Non-vertical slab motions, which occur prior to break-off, represent a potentially significant source of error for slab-based plate reconstructions, but are poorly understood. We constrain lateral migration of the Indian slab and overlying India-Asia collision zone by comparing tomographically-imaged mantle structure with plate-kinematic constraints. Following coupling of the Indian and Australian plates at the onset of collision, ~1000 km lateral migration of the Indian slab was driven by vertical subduction of the Australian slab. The sinking behaviours of individual slabs do not evolve in isolation, but instead influence, or are influenced by, other slabs in the same plate network. Hence, lateral slab migrations may be determined by interpreting the sinking behaviour of slabs collectively, and with respect to plate kinematics.

The ultimate goal of tectonic plate reconstruction modelling is to constrain absolute motions of Earth's continents and oceans, with respect to the mantle, through geological time (Torsvik et al., 2008, van der Meer et al., 2010, Doubrovine et al., 2012). This is crucial to our understanding of how surface processes, plate tectonics, and mantle dynamics link at a planetary scale (Steinberger et al., 2012, Domeier et al., 2016), and essential for the ability to test working hypotheses against bedrock and mantle records (Wu et al., 2016, Sigloch and Mihalynuk, 2017, van de Lagemaat et al., 2018, Clennett et al., 2020, Fuston and Wu, 2020, Parsons et al., 2020). Absolute plate motions are constrained using a mantle reference frame, based primarily on the tracking of oceanic plates across mantle hot-spots (Torsvik et al., 2008, Doubrovine et al., 2012). However, hot-spot tracks do not extend beyond ~130 Ma, which increases the uncertainty of absolute reconstructions of earlier times (Doubrovine et al., 2012, Domeier et al., 2016). Development of a mantle reference frame that uses subducted slabs as fixed reference points is a highly desirable solution to this problem, because the widespread distribution and longer-term residency of slabs in the lower mantle should allow us to reconstruct absolute plate motions with greater accuracy, back to at least 200-300 Ma (van der Meer et al., 2010, Steinberger et al., 2012, Domeier et al., 2016, van der Meer et al., 2018).

Tomographically constrained, slab-based plate reconstructions are typically founded on an assumption that after slab break-off, detached slabs sink vertically, such that the top of a detached slab constrains the surface location of its subduction zone trench, at point of break-off (Hafkenscheid et al., 2006, van der Meer et al., 2010, Steinberger et al., 2012, Replumaz et al., 2014, Domeier et al., 2016, Wu et al., 2016, Parsons et al., 2020). Prior to slab break-off, the potential for horizontal slab motions *during* subduction is poorly constrained, but has been shown to produce significant errors in slab-based reconstructions if overlooked (Schellart, 2005, van de Lagemaat et al., 2018).

Lateral slab migration (LSM) refers to a horizontal component of motion of part of, or all of, a slab, which occurs during subduction, prior to slab break-off, and with respect to the surrounding mantle. Numerical and analogue modelling suggest that LSM can occur in the upper mantle, where the viscosity of a slab may force it to migrate perpendicular to the trench, towards or away from the direction of subduction, as the slab bends and steepens (Schellart, 2005, Schellart et al., 2008, Capitanio and Morra, 2012, Čížková and Bina, 2013, Holt et al., 2018). Such migrations are predicted on the order of a few hundreds of kilometres and are typically accompanied by trench migration (Schellart, 2005, Schellart et al., 2008, Holt et al., 2018). Within the lower mantle, modelling suggests that slabs sink vertically (Steinberger et al., 2012, Čížková and Bina, 2013) with minor LSM on the order of ~100-200 km per 100 Myrs (Steinberger et al., 2012).

LSMs inferred from observations of subducted slabs are uncommon (Le Dain et al., 1984, Giardini and Woodhouse, 1986, Liu et al., 2008, Spakman et al., 2018, van de Lagemaat et al., 2018), and in some cases disputed (Liu et al., 2008, Sigloch and Mihalynuk, 2017). Most notably, van de Lagemaat et al. (2018) demonstrate ~1200 km of trench-parallel LSM of the Pacific slab beneath the Kermadec arc since ~30 Ma, which was previously unaccounted for by plate reconstructions. Importantly, magnitudes and directions of LSM inferred from natural examples have been shown to correspond to absolute plate motion of the subducting plate (Spakman et al., 2018, van de Lagemaat et al., 2018). This implies that within a single plate network, slab sinking (prior to break-off) and absolute plate motions are related to each other. If this is correct, it should be possible to constrain components of LSM from multiple slabs of the same network, by interpreting their sinking kinematics collectively, and as connected parts that maintain compatibility with plate kinematics during subduction. To test this hypothesis, we investigate the subduction kinematics of the India-Asia collision (Fig. 1), where LSM has been proposed previously, but not constrained (Le Dain et al., 1984, Parsons et al., 2020). We integrate seismic tomography (Fig. 2) with bedrock and plate-kinematic constraints to constrain the kinematics of the Australian and Indian slabs during the India-Asia collision (Fig. 3). By interpreting the size, distribution and morphology of these slabs collectively, we propose that subduction of the Australian slab provided the driving force for ~1000 km northward LSM of the Indian slab (Fig. 4).

Plate network configurations for the India-Asia collision

Several hypotheses have been proposed for the India-Asia collision, which vary in terms of timing and number of collisions. Single-collision hypotheses propose a single, continuous collision between India and Asia, which initiated at 59 ± 1 Ma (Hu et al., 2016, Ingalls et al., 2016). Double-collision hypotheses argue for distinct collisional events at 59 ± 1 Ma (“First Collision”) and ~45-40 Ma (“Second Collision”) (Patriat and Achache, 1984, Bouilhol et al., 2013, Jagoutz et al., 2015, van Hinsbergen et al., 2019). Double-collision Hypothesis I proposes “First Collision” between India and an equatorial intra-oceanic arc, followed by “Second Collision” between India-plus-arc and Eurasia (Patriat and Achache, 1984, Bouilhol et al., 2013, Jagoutz et al., 2015). Double-collision Hypothesis II proposes “First Collision” between an India-derived microcontinent and Eurasia, followed by “Second Collision” between India and the modified Eurasian margin (van Hinsbergen et al., 2019). Based on the review of Parsons et al. (2020), our study analyses slab kinematics during the India-Asia collision in the context of double-collision hypotheses I and II (Fig. 3) (Patriat and Achache, 1984,

Bouilhol et al., 2013, Jagoutz et al., 2015, van Hinsbergen et al., 2019). Single-collision hypotheses require extreme magnitudes of continental subduction, do not fit restorations of Gondwana, offer no explanation for the plate network reorganization at 45-40 Ma (detailed below), and are not considered further (Parsons et al., 2020).

Between ~120-40 Ma, the Indian plate was bounded by north-south striking transform boundaries to its west and east (Fig. 3); its eastern boundary, defined by the Wharton ridge (Fig. 1), formed a transform-dominated spreading ridge (Jacob et al., 2014, Gibbons et al., 2015). During that period, the adjacent Australian plate remained at a relatively fixed position (Torsvik et al., 2008). Bedrock records along the southern Eurasian margin reflect the contrasting kinematics of the Indian and Australian plates (Fig. 1). West of the Wharton ridge, subduction-related magmatism between southwest Tibet and Thailand occurred throughout the Late Cretaceous to ~50-40 Ma (Morley, 2012, Zhu et al., 2018, Lin et al., 2019). East of the Wharton ridge, northward subduction beneath Java and Sulawesi ceased at ~90-80 Ma (Hall, 2012, Morley, 2012, Breithfeld et al., 2020), and re-initiated beneath Java at 47-44 Ma (Smyth et al., 2008), coincident with onset of northward migration of the Australian plate (Torsvik et al., 2008, Müller et al., 2019).

During the mid-Eocene, a significant plate network reorganization was recorded across the Indian Ocean (Patriat and Achache, 1984, Gibbons et al., 2015) (Fig. 3c). This included: (1) 30-38% reduction in Indian plate velocity between 45-40 Ma (Molnar and Stock, 2009); (2) cessation of Wharton ridge spreading and subsequent coupling between Indian and Australian plates at ~43-36 Ma (Jacob et al., 2014, Gibbons et al., 2015); (3) onset of Australian plate subduction beneath Java at 47-44 Ma (Smyth et al., 2008); (4) onset of northward migration of the Australian plate at ~45-43 Ma (Torsvik et al., 2008, Müller et al., 2019); (5) accelerated spreading between the Australian and Antarctic plates at ~47-45 Ma (Torsvik et al., 2008, Eagles, 2019, Seton et al., 2020); (6) change in rates and azimuths of spreading between India and Africa between 47-41 Ma (Patriat and Achache, 1984, Cande et al., 2010, Seton et al., 2020); (7) southwestward jump of the Central India spreading ridge at ~41 Ma (Torsvik et al., 2013). These well-constrained changes in plate kinematics and subduction make the Indian and Australian plates and associated slabs a good target for testing whether LSMs can be inferred by interpreting the kinematics of multiple slabs collectively, and with respect to plate motions.

Slab kinematics during the India-Asia collision

We focus on two slabs of subducted lithosphere beneath southeast Asia (Anomaly VII) and northern India (Anomaly II; *anomaly numbers follow Parsons et al., 2020*) (Fig. 2), based on combined observations from six tomography models (Supporting Information and Dataset) (Amaru, 2007, Li et al., 2008a, Simmons et al., 2012, Obayashi et al., 2013, Schaeffer and Lebedev, 2013, Hosseini et al., 2020). Our interpretations of these slabs are supported by the most up-to-date, integrated assessment of bedrock, subsurface and kinematic constraints from Tibet-Himalaya and central Indian Ocean (Parsons et al., 2020). Further constraints are provided by our own integration of bedrock and mantle records between Myanmar and Indonesia, and Australian plate kinematics (see Supporting Information), which were not considered by previous tomographically-constrained interpretations of the study region (Hafkenscheid et al., 2006; Replumaz et al., 2014; Parsons et al., 2020).

Anomaly VII comprises Indian and Australian lithosphere presently subducting between Myanmar and Indonesia and includes the extinct Wharton ridge (Figs. 1-2). Between Sumatra and Indonesia, Anomaly VII forms a near-vertical slab from the trench down to ~800-1000 km depth, where it thickens as it piles up in the mantle transition zone (MTZ) and lower mantle (Figs. 2i, S2j-q). Beneath Myanmar and Thailand, Anomaly VII dips southwards (Fig. 2h). Parts of this western section of Anomaly VII are doubly thickened with respect to its eastern section (Fig. S2i).

Anomaly II is a detached slab imaged in the MTZ and lower mantle beneath Tibet and northern India (Fig. 2). Between ~450–550 km and ~800-1000 km depth, Anomaly IIa forms a NW-SE striking, southwest dipping, linear anomaly (Fig. 2a). Between ~800-1000 km and ~1100-1300 km depth, Anomaly IIb forms a wider, subhorizontal anomaly (Figs. 2b-d, 2g-h, S2e-g).

We integrate our analysis of Anomalies VII and II within a kinematic reconstruction of the Indian, Australian and Eurasian plates at 59 Ma and 43 Ma (Fig. 3), corresponding to “First” and “Second” collision, respectively (Patriat and Achache, 1984, Bouilhol et al., 2013). Our 59 Ma restoration (Fig. 3b) includes alternative plate-boundary configurations for both double-collision hypotheses (Patriat and Achache, 1984, Bouilhol et al., 2013, Jagoutz et al., 2015, van Hinsbergen et al., 2019). Indian and Australian plate motions are constrained by seafloor isochrons in a moving-hotspot reference frame (Müller et al., 2019). The location and kinematics of the southern Eurasian subduction zone are constrained from our tomography analysis (Figs. 2, S2-4), integrated with bedrock and plate-kinematic constraints (Supporting Information).

First, we focus on the kinematics of the Anomaly VII slab (beneath Myanmar to Indonesia). The well-defined morphology of Anomaly VII and its connectivity with the Indian and Australian plates (Figs 2i, S2h-q) make it suitable for restoration to its pre-subduction horizontal length following methods outlined by Hafkenscheid et al. (2006) and Wu et al. (2016) (methods detailed in supporting information).

Figure 3a shows our maximum and minimum restored lengths of the Anomaly VII slab determined from cross sections H to Q. Between cross sections J to Q, the length of lithosphere restored from Anomaly VII (distance between yellow dots and grey-white dashed lines) is equivalent to the total plate motion of the Australian plate, since ~43 Ma (Torsvik et al., 2008, Müller et al., 2019) (distance between yellow and red dots). This equivalency between Anomaly VII slab volume and Australian plate motion since ~43 Ma implies that Anomaly VII is not voluminous enough to account for subduction beneath the southeast Eurasian margin *prior* to ~43 Ma. This geometry-based inference is independent of, but consistent with (1) Late Cretaceous-Middle Eocene hiatus of subduction beneath southeast Eurasia (Hall, 2012, Morley, 2012) during a period of relative immobility of the Australian plate (Torsvik et al., 2008, Müller et al., 2019); followed by (2) onset of subduction beneath Java (Smyth et al., 2008) and northward migration of the Australian plate (Torsvik et al., 2008, Müller et al., 2019) at 47-43 Ma (Fig. 3c). Integrating these events with our restoration of Anomaly VII suggests that the Eurasian margin between sections J to Q has been stationary since ~90-80 Ma (Fig. 3a). This is consistent with the vertical morphology of Anomaly VII between sections J to Q (Fig. 2i), which is most simply explained by subduction beneath a stationary trench with negligible LSM. We therefore carry over our 43 Ma restoration of the Eurasian margin between sections J to Q into our 59 Ma restoration (Fig. 3b).

On cross sections H and I, we interpret the southwards dip (Fig. 2h) and thickened geometry (Fig. S2i) of Anomaly VII as a record of slab overturning (e.g. Schellart, 2005, Capitanio et al., 2015), caused by northwards trench migration, during subduction. Assuming that the slab sank vertically as it overturned, the southern basal edge of the slab marks the approximate location of the overlying trench at the onset of subduction. From this, we estimate that since ~43 Ma, the Sunda-Andaman trench has migrated ~800 km and ~300 km northeast along sections H (Fig. 2h) and I (Fig. S2i), respectively. Incorporating our estimates of trench migration into our restoration demonstrates an equivalency between Indian plate motion since ~43 Ma (distance between yellow and red dots) and the combined length of [restored Anomaly VII slab] + [trench migration] from sections H and I (distance between yellow dots and light blue-white dashed lines). Thus, at 43 Ma, we restore the Sunda-Andaman trench overlying sections H and I, 800 km and 300 km southeast of its present day location (orange dots, Fig 3a), along strike from the restored Eurasian margin between sections J to Q.

Crucially, the restored 43 Ma Eurasian margin between sections H and I (orange dots, Fig. 3a) coincides *spatially* with the reconstructed northern edge of Greater India (Fig. 3a) (constrained by Parsons et al., 2020), and *temporally* with the 30-38% reduction in Indian plate velocity between ~45-40 Ma (Molnar and Stock, 2009) (Fig. 3c). Hence, our restoration supports previous arguments (Patriat and Achache, 1984, Bouilhol et al., 2013, Gibbons et al., 2015, Jagoutz et al., 2015) that collision between India and Eurasia occurred at ~45-40 Ma (Fig. 3c). We therefore propose that at 43 Ma, the northern edge of Greater India was in contact with the Eurasian margin, and so we extend our Eurasian margin restoration (red barbed line, Fig. 3a) westward from section H, coincident with the edge of Greater India. Our restoration implies that since collision at ~43 Ma, the India-Eurasia plate boundary west of section H has migrated ~1000-2000 km northeast to its present-day location, defined by the Indus suture zone (ISZ, Fig. 3a). This is consistent with paleomagnetic constraints which place southern Tibet at $20^{\circ}\text{N} \pm 4^{\circ}$ at ~52 Ma (Huang et al., 2015). A shapefile of our Eurasian margin restoration is included in supplementary files.

We attribute differences in trench kinematics and slab morphology between sections H to I, and J to Q, to the Wharton ridge, which we restore coincident with section J at 43 Ma and 59 Ma (Fig. 3a-b). The Eurasian margin at sections H and I formed part of the longer lived subduction zone between Myanmar-Thailand and southern Tibet that was responsible for subduction of the Indian \pm Neotethys plate(s) from ~110 Ma to ~40 Ma (Zhu et al., 2018, Lin et al., 2019) (Fig. 3b). The corresponding slab(s) associated with that subduction began subducting ~70 Myr earlier than the Anomaly VII slab (Fig 3b), and hence should now be located deeper than Anomaly VII. We therefore assign the Indian plate slab to Anomaly II (Fig. 3b), imaged beneath north India from ~450-550 km to ~1000-1300 km depth (Fig. 2a-c,g-h). We are confident in this interpretation because it is the simplest explanation for the whereabouts of the Indian plate slab, and because there are no other oceanic basins that Anomaly II can be related to (Parsons et al., 2020).

Importantly, Anomaly II is presently located ~1000 km north of our 43 Ma restoration of the Eurasian margin (Figs. 2g, 3a). Applying an assumption of vertical sinking with no LSM to Anomaly II would contradict our restorations of the Eurasian and Indian margins, and from a kinematic perspective, would delay contact between India and Eurasia by ~10-20 Myrs. We therefore propose that since “Second Collision” at ~45-40 Ma, the Anomaly II slab has laterally migrated ~1000 km

northwards through the surrounding mantle (Figs 2g, 4). The south dipping morphology of Anomaly II is consistent with slab-overturning during LSM (Figs. 2g, S2e-g).

Previous studies that did not consider the sinking kinematics of Anomaly VII in their investigations of Anomaly II, did not detect LSM (Hafkenscheid et al., 2006, Replumaz et al., 2014). Instead, those studies either located the ~60-45 Ma collision zone above present-day Anomaly II (Hafkenscheid et al., 2006), which is inconsistent with the location of the northern Indian margin at that time (Fig. 3a-b), or interpreted Anomaly II as subducted Indian and Asian *continental* lithosphere (Replumaz et al., 2014), which is not robustly demonstrated by bedrock and geophysical observations (Parsons et al. 2020). Interpreting the Indian slab (Anomaly II) with respect to the Australian slab (Anomaly VII) and the surrounding plate network, as we do, leads us to our new interpretation, which is supported by a greater set of constraints.

Lastly, we note that our Eurasian margin restoration (red barbed line, Fig. 3a-b) is coincident with Anomaly III (grey-dashed line, Fig. 3a), which forms a vertical slab-wall from ~800-950 km to ~1700-1800 km depth (Fig. 2). We therefore propose that the southern Eurasian plate boundary formed a subduction zone above Anomaly III, tens of millions of years prior to 59 Ma (Fig. 3b).

Plate tectonic explanation for LSMs

Our analysis suggests that east of the Wharton ridge, the Eurasian margin and Anomaly VII slab remained at a relatively fixed location since ~43 Ma. At the same time, west of the Wharton ridge, the Anomaly II slab laterally displaced by ~1000 km, and the Anomaly VII slab overturned as the overlying India-Asia collision zone migrated ~1000-2000 km northwards (Fig. 4).

Our interpretation is consistent with numerical models, which propose northward migration of the India-Asia collision zone was driven by Australian plate subduction (e.g. Capitanio et al., 2015). Consistent with those models, we propose that following Second Collision at ~45-40 Ma (Fig. 4a), wholesale motion of the newly coupled India-Australia plate was driven by slab-pull of the subducting Australian oceanic lithosphere (Anomaly VII-Aus, Fig. 4) (e.g. Li et al., 2008b, Capitanio et al., 2015), whilst to the west, buoyancy of the Indian continent stalled Indian-plate subduction (Fig. 4a-c). To maintain compatibility between slab kinematics and plate kinematics, the Indian continent was forced northwards, dragging the Indian oceanic slab with it (Anomaly II, Fig. 4b-c). Within the mantle, the laterally migrating Indian slab (Anomaly II) separated from the vertically sinking Australian oceanic slab (Anomaly VII-Aus, Fig. 4b-c) along the subducted portion of the Wharton ridge (Fig. 4b-c).

During northward migration of the Anomaly II slab and the India-Asia collision zone, Indian oceanic lithosphere between India and the Wharton ridge overturned during subduction (Anomaly VII-Ind, Figs. 2i, 4b-c), whilst the overlying subduction zone between Myanmar and Sumatra rotated clockwise (around a vertical axis) and lengthened via NW-SE transform faulting (Fig. 4a-c). We interpret the present-day location of Anomaly II as the location of complete Indian slab break-off from the Indian continent, corresponding to a restoration age of ~30-25 Ma (Fig. 4b-c).

We build upon the observations of Replumaz et al. (2014), who recognised an overturned slab in the upper mantle beneath India, by *kinematically* demonstrating that (1) Anomaly II is an oceanic slab, which was dragged ~1000 km northwards during collision; and (2) timing and duration of Anomaly II

LSM coincided with the timing and duration of Australian plate subduction. Our study also demonstrates that onset of subduction of the Australian plate coincided with plate network reorganization in the Indian Ocean (Fig. 3c), including: (1) reorientation of Indian plate-motion azimuth, from 000-020° to 020-040° (Torsvik et al., 2008, Gibbons et al., 2015, Müller et al., 2019); and (2) changes in rates and azimuths of spreading between the Indian and African plates (Patriat and Achache, 1984, Cande et al., 2010, Torsvik et al., 2013, Seton et al., 2020) and between the Australian and Antarctic plates (Torsvik et al., 2008, Eagles, 2019, Seton et al., 2020) (Fig. 3c). Based on an understanding that slab-pull is the dominant force behind plate motions (Forsyth and Uyeda, 1975), we postulate that these kinematic changes occurred in response to the onset of Australian slab subduction.

Conclusions

We believe this is the first kinematically-constrained demonstration of significant LSM reported (1) from a now-detached slab; and (2) in a trench-forward direction. Our findings demonstrate that magnitudes of LSM prior to slab break-off can be large, and will produce errors in slab-based plate reconstructions if overlooked. An assumption of vertical sinking applied to the Indian slab (Anomaly II) would reconstruct the Eurasian margin directly above Anomaly II, which is incompatible with our interpretation of the Australian slab (Anomaly VII), our restoration of the Eurasian and Indian margins, and from a kinematic perspective, would delay collision by ~10-20 Myrs. Instead, we have demonstrated that the Indian slab migrated ~1000 km laterally through the mantle since collision between India and Eurasia at 45-40 Ma.

Previous studies, did not detect LSM because they did not consider the kinematics of Anomaly VII (Australian slab) in their interpretations of Anomaly II (Indian slab). We arrive at our new interpretation because, (1) we interpreted the distribution and geometry of subducted slabs as integrated parts of a larger system (rather than in isolation); and (2) we expanded our region of interest to include the Myanmar-to-Indonesia margin and Australian plate kinematics, to ensure that our interpretations maintained compatibility between slab kinematics and plate kinematics.

Acknowledgements

For the purpose of review, data presented in this study are available in the supporting information. Upon acceptance, data presented in this study will be hosted and made freely available at the Oxford University Research Archive (ORA). We thank editor Lucy Flesch and reviewers Jon Pownall and Fabio Capitanio for constructive reviews that improved our study. We thank Jonny Wu and Richard Palin for helpful discussions regarding slab densities and slab area to plate area conversions. We thank Graeme Eagles and Lucia Perez-Diaz for helpful discussions regarding the plate tectonic evolution of the Indian Ocean. This work was supported by funding from the European Research Council (ERC) under the European Union's Horizon 2020 research and innovation programme (grant agreement 639003 "DEEP TIME").

- Amaru, M. 2007. *Global travel time tomography with 3-D reference models*. Utrecht University.
- Barber, A.J., Khin Zaw & Crow, M.J. 2017. Chapter 31: The pre-Cenozoic tectonic evolution of Myanmar. In: Barber, A. J., Khin Zaw & Crow, M. J. (eds.) *Myanmar: Geology, Resources and Tectonics*. Geological Society, London, Memoirs, 48, 687-712.
- Barley, M.E., Pickard, A.L., Zaw, K., Rak, P. & Doyle, M.G. 2003. Jurassic to Miocene magmatism and metamorphism in the Mogok metamorphic belt and the India-Eurasia collision in Myanmar. *Tectonics*, 22.
- Bergman, S.C., Coffield, D.Q., Talbot, J.P. & Garrard, R.A. 1996. Tertiary Tectonic and magmatic evolution of western Sulawesi and the Makassar Strait, Indonesia: evidence for a Miocene continent-continent collision. *Geological Society, London, Special Publications*, 106, 391-429.
- Bertrand, G., Rangin, C., Maluski, H. & Bellon, H. 2001. Diachronous cooling along the Mogok Metamorphic Belt (Shan scarp, Myanmar): the trace of the northward migration of the Indian syntaxis. *Journal of Asian Earth Sciences*, 19, 649-659.
- Bertrand, G. & Rangin, C. 2003. Tectonics of the western margin of the Shan plateau (central Myanmar): implication for the India–Indochina oblique convergence since the Oligocene. *Journal of Asian Earth Sciences*, 21, 1139-1157.
- Bird, P. 2003. An updated digital model of plate boundaries. *Geochemistry, Geophysics, Geosystems*, 4.
- Bouilhol, P., Jagoutz, O., Hanchar, J.M. & Dudas, F.O. 2013. Dating the India–Eurasia collision through arc magmatic records. *Earth and Planetary Science Letters*, 366, 163-175.
- Breitfeld, H.T., Davies, L., Hall, R., Armstrong, R., Forster, M., Lister, G., Thirlwall, M., Grassineau, N., Hennig-Breitfeld, J. & van Hattum, M.W.A. 2020. Mesozoic Paleo-Pacific Subduction Beneath SW Borneo: U-Pb Geochronology of the Schwaner Granitoids and the Pinoh Metamorphic Group. *Frontiers in Earth Science*, 8.
- Brook, M. & Snelling, N. 1976. K/Ar and Rb/Sr age determinations on rocks and minerals from Burma. *Report of the Isotope Geology Unit*, 76, 12.
- Burg, J.-P. & Bouilhol, P. 2018. Timeline of the South-Tibet--Himalayan belt: the geochronological record of subduction, collision, and underthrusting from zircon and monazite U-Pb ages. *Canadian Journal of Earth Sciences*.
- Cande, S.C., Patriat, P. & Dymant, J. 2010. Motion between the Indian, Antarctic and African plates in the early Cenozoic. *Geophysical Journal International*, 183, 127-149.
- Capitanio, F.A. & Morra, G. 2012. The bending mechanics in a dynamic subduction system: Constraints from numerical modelling and global compilation analysis. *Tectonophysics*, 522-523, 224-234.
- Capitanio, F.A., Replumaz, A. & Riel, N. 2015. Reconciling subduction dynamics during Tethys closure with large-scale Asian tectonics: Insights from numerical modeling. *Geochemistry, Geophysics, Geosystems*, 16, 962-982.
- Čížková, H. & Bina, C.R. 2013. Effects of mantle and subduction-interface rheologies on slab stagnation and trench rollback. *Earth and Planetary Science Letters*, 379, 95-103.
- Clennett, E.J., Sigloch, K., Mihalynuk, M.G., Seton, M., Henderson, M.A., Hosseini, K., Mohammadzaheri, A., Johnston, S.T. & Müller, R.D. 2020. A Quantitative Tomotectonic Plate Reconstruction of Western North America and the Eastern Pacific Basin. *Geochemistry, Geophysics, Geosystems*, 21, e2020GC009117.
- Crow, M.J. & Khin Zaw 2017. Appendix: Geochronology in Myanmar (1964–2017). In: Barber, A. J., Zaw, K. & Crow, M. J. (eds.) *Myanmar: Geology, Resources and Tectonics*. Geological Society, London, Memoirs. 48, 713-759.
- Domeier, M., Doubrovine, P.V., Torsvik, T.H., Spakman, W. & Bull, A.L. 2016. Global correlation of lower mantle structure and past subduction. *Geophysical Research Letters*, 43, 4945-4953.
- Doubrovine, P.V., Steinberger, B. & Torsvik, T.H. 2012. Absolute plate motions in a reference frame defined by moving hot spots in the Pacific, Atlantic, and Indian oceans. *Journal of Geophysical Research: Solid Earth*, 117.

- Dziewonski, A.M. & Anderson, D.L. 1981. Preliminary reference Earth model. *Physics of the Earth and Planetary Interiors*, 25, 297-356.
- Eagles, G. 2019. A little spin in the Indian Ocean plate circuit. *Tectonophysics*, 754, 80-100.
- Forsyth, D. & Uyeda, S. 1975. On the Relative Importance of the Driving Forces of Plate Motion*. *Geophysical Journal of the Royal Astronomical Society*, 43, 163-200.
- Fuston, S. & Wu, J. 2020. Raising the Resurrection plate from an unfolded-slab plate tectonic reconstruction of northwestern North America since early Cenozoic time. *GSA Bulletin*.
- Gardiner, N.J., Roberts, N.M.W., Morley, C.K., Searle, M.P. & Whitehouse, M.J. 2016a. Did Oligocene crustal thickening precede basin development in northern Thailand? A geochronological reassessment of Doi Inthanon and Doi Suthep. *Lithos*, 240-243, 69-83.
- Gardiner, N.J., Searle, M.P., Morley, C.K., Whitehouse, M.P., Spencer, C.J. & Robb, L.J. 2016b. The closure of Palaeo-Tethys in Eastern Myanmar and Northern Thailand: New insights from zircon U–Pb and Hf isotope data. *Gondwana Research*, 39, 401-422.
- Gardiner, N.J., Searle, M.P., Morley, C.K., Robb, L.J., Whitehouse, M.J., Roberts, N.M.W., Kirkland, C.L. & Spencer, C.J. 2018. The crustal architecture of Myanmar imaged through zircon U-Pb, Lu-Hf and O isotopes: Tectonic and metallogenic implications. *Gondwana Research*, 62, 27-60.
- Giardini, D. & Woodhouse, J.H. 1986. Horizontal shear flow in the mantle beneath the Tonga arc. *Nature*, 319, 551-555.
- Gibbons, A.D., Zahirovic, S., Müller, R.D., Whittaker, J.M. & Yatheesh, V. 2015. A tectonic model reconciling evidence for the collisions between India, Eurasia and intra-oceanic arcs of the central-eastern Tethys. *Gondwana Research*, 28, 451-492.
- Guan, Q., Zhu, D.-C., Zhao, Z.-D., Dong, G.-C., Zhang, L.-L., Li, X.-W., Liu, M., Mo, X.-X., Liu, Y.-S. & Yuan, H.-L. 2012. Crustal thickening prior to 38Ma in southern Tibet: Evidence from lower crust-derived adakitic magmatism in the Gangdese Batholith. *Gondwana Research*, 21, 88-99.
- Hafkenscheid, E., Wortel, M.J.R. & Spakman, W. 2006. Subduction history of the Tethyan region derived from seismic tomography and tectonic reconstructions. *Journal of Geophysical Research: Solid Earth*, 111, n/a-n/a.
- Hall, R. 2012. Late Jurassic–Cenozoic reconstructions of the Indonesian region and the Indian Ocean. *Tectonophysics*, 570-571, 1-41.
- Haproff, P.J., Zuza, A.V., Yin, A., Harrison, T.M., Manning, C.E., Dubey, C.S., Ding, L., Wu, C. & Chen, J. 2019. Geologic framework of the northern Indo-Burma Ranges and lateral correlation of Himalayan-Tibetan lithologic units across the eastern Himalayan syntaxis. *Geosphere*, 15, 856-881.
- Haproff, P.J., Odlum, M.L., Zuza, A.V., Yin, A. & Stockli, D.F. 2020. Structural and Thermochronologic Constraints on the Cenozoic Tectonic Development of the Northern Indo-Burma Ranges. *Tectonics*, 39, e2020TC006231.
- Hayes, G.P., Moore, G.L., Portner, D.E., Hearne, M., Flamme, H., Furtney, M. & Smoczyk, G.M. 2018. Slab2, a comprehensive subduction zone geometry model. *Science*, 362, 58-61.
- Hennig, J., Hall, R. & Armstrong, R.A. 2016. U-Pb zircon geochronology of rocks from west Central Sulawesi, Indonesia: Extension-related metamorphism and magmatism during the early stages of mountain building. *Gondwana Research*, 32, 41-63.
- Holt, A.F., Royden, L.H., Becker, T.W. & Faccenna, C. 2018. Slab interactions in 3-D subduction settings: The Philippine Sea Plate region. *Earth and Planetary Science Letters*, 489, 72-83.
- Hosseini, K., Matthews, K.J., Sigloch, K., Shephard, G.E., Domeier, M. & Tsekhmistrenko, M. 2018. SubMachine: Web-Based Tools for Exploring Seismic Tomography and Other Models of Earth's Deep Interior. *Geochemistry, Geophysics, Geosystems*, 19, 1464-1483.
- Hosseini, K., Sigloch, K., Tsekhmistrenko, M., Zaheri, A., Nissen-Meyer, T. & Igel, H. 2020. Global mantle structure from multi-frequency tomography using P, PP and P-diffracted waves. *Geophysical Journal International*, 220, 96-141.

- Hu, X., Garzanti, E., Wang, J., Huang, W., An, W. & Webb, A. 2016. The timing of India-Asia collision onset – Facts, theories, controversies. *Earth-Science Reviews*, 160, 264-299.
- Huang, W., Dupont-Nivet, G., Lippert, P.C., Hinsbergen, D.J.J., Dekkers, M.J., Waldrup, R., Ganerød, M., Li, X., Guo, Z. & Kapp, P. 2015. What was the Paleogene latitude of the Lhasa terrane? A reassessment of the geochronology and paleomagnetism of Linzizong volcanic rocks (Linzhou basin, Tibet). *Tectonics*, 34, 594-622.
- Ingalls, M., Rowley, D.B., Currie, B. & Colman, A.S. 2016. Large-scale subduction of continental crust implied by India–Asia mass-balance calculation. *Nature Geoscience*, 9, 848.
- Jacob, J., Dymment, J. & Yatheesh, V. 2014. Revisiting the structure, age, and evolution of the Wharton Basin to better understand subduction under Indonesia. *Journal of Geophysical Research: Solid Earth*, 119, 169-190.
- Jagoutz, O., Royden, L., Holt, A.F. & Becker, T.W. 2015. Anomalously fast convergence of India and Eurasia caused by double subduction. *Nature Geoscience*, 8, 475.
- Jagoutz, O., Bouilhol, P., Schaltegger, U. & Müntener, O. 2018. The isotopic evolution of the Kohistan Ladakh arc from subduction initiation to continent arc collision. *Geological Society, London, Special Publications*, 483.
- Khin, K., Zaw, K., Aung, L.T., Barber, A.J., Zaw, K. & Crow, M.J. 2017. Geological and tectonic evolution of the Indo-Myanmar Ranges (IMR) in the Myanmar region. In: Barber, A. J., Zaw, K. & Crow, M. J. (eds.) *Myanmar: Geology, Resources and Tectonics*. The Geological Society of London. 48, 65-79.
- Lamont, T.N., Searle, M.P., Hacker, B.R., Htun, K., Htun, K.M., Morley, C.K., Waters, D.J. & White, R.W. 2021. Late Eocene-Oligocene granulite facies garnet-sillimanite migmatites from the Mogok Metamorphic belt, Myanmar, and implications for timing of slip along the Sagaing Fault. *Lithos*, 106027.
- Le Dain, A.Y., Tapponnier, P. & Molnar, P. 1984. Active faulting and tectonics of Burma and surrounding regions. *Journal of Geophysical Research: Solid Earth*, 89, 453-472.
- Li, C., van der Hilst, R.D., Engdahl, E.R. & Burdick, S. 2008a. A new global model for P wave speed variations in Earth's mantle. *Geochemistry, Geophysics, Geosystems*, 9.
- Li, C., van der Hilst, R.D., Meltzer, A.S. & Engdahl, E.R. 2008b. Subduction of the Indian lithosphere beneath the Tibetan Plateau and Burma. *Earth and Planetary Science Letters*, 274, 157-168.
- Li, Z., Ding, L., Zaw, T., Wang, H., Cai, F., Yao, W., Xiong, Z., Sein, K. & Yue, Y. 2020. Kinematic evolution of the West Burma block during and after India-Asia collision revealed by paleomagnetism. *Journal of Geodynamics*, 134, 101690.
- Licht, A., Dupont-Nivet, G., Win, Z., Swe, H.H., Kaythi, M., Roperch, P., Ugrai, T., Littell, V., Park, D., Westerweel, J., Jones, D., Poblete, F., Aung, D.W., Huang, H., Hoorn, C. & Sein, K. 2018. Paleogene evolution of the Burmese forearc basin and implications for the history of India-Asia convergence. *GSA Bulletin*, 131, 730-748.
- Licht, A., Win, Z., Westerweel, J., Cogné, N., Morley, C.K., Chantpraserst, S., Poblete, F., Ugrai, T., Nelson, B., Aung, D.W. & Dupont-Nivet, G. 2020. Magmatic history of central Myanmar and implications for the evolution of the Burma Terrane. *Gondwana Research*, 87, 303-319.
- Lin, T.-H., Mitchell, A.H.G., Chung, S.-L., Tan, X.-B., Tang, J.-T., Oo, T. & Wu, F.-Y. 2019. Two parallel magmatic belts with contrasting isotopic characteristics from southern Tibet to Myanmar: zircon U–Pb and Hf isotopic constraints. *Journal of the Geological Society*, 176, 574-587.
- Liu, L., Spasojević, S. & Gurnis, M. 2008. Reconstructing Farallon Plate Subduction Beneath North America Back to the Late Cretaceous. *Science*, 322, 934-938.
- Ma, L., Wang, B.-D., Jiang, Z.-Q., Wang, Q., Li, Z.-X., Wyman, D.A., Zhao, S.-R., Yang, J.-H., Gou, G.-N. & Guo, H.-F. 2014. Petrogenesis of the Early Eocene adakitic rocks in the Napuri area, southern Lhasa: Partial melting of thickened lower crust during slab break-off and implications for crustal thickening in southern Tibet. *Lithos*, 196-197, 321-338.
- Macdonald, A.S., Barr, S.M., Miller, B.V., Reynolds, P.H., Rhodes, B.P. & Yokart, B. 2010. P–T–t constraints on the development of the Doi Inthanon metamorphic core complex domain and

- implications for the evolution of the western gneiss belt, northern Thailand. *Journal of Asian Earth Sciences*, 37, 82-104.
- Martin, C.R., Jagoutz, O., Upadhyay, R., Royden, L.H., Eddy, M.P., Bailey, E., Nichols, C.I.O. & Weiss, B.P. 2020. Paleocene latitude of the Kohistan–Ladakh arc indicates multistage India–Eurasia collision. *Proceedings of the National Academy of Sciences*, 117, 29487-29494.
- Matthews, K.J., Maloney, K.T., Zahirovic, S., Williams, S.E., Seton, M. & Müller, R.D. 2016. Global plate boundary evolution and kinematics since the late Paleozoic. *Global and Planetary Change*, 146, 226-250.
- Min, M. 2007. *Thermochronology applied to strike-slip zones Central America and Myanmar*. PhD thesis.
- Min, S., Watkinson, I.M., Tun, S.T., Naing, W. & Swe, T.L. 2017. The Kyaukkyan Fault, Myanmar. In: Barber, A. J., Zaw, K. & Crow, M. J. (eds.) *Myanmar: Geology, Resources and Tectonics*. The Geological Society of London. 48, 453-471.
- Molnar, P. & Stock, J.M. 2009. Slowing of India's convergence with Eurasia since 20 Ma and its implications for Tibetan mantle dynamics. *Tectonics*, 28.
- Morley, C.K. 2012. Late Cretaceous–Early Palaeogene tectonic development of SE Asia. *Earth-Science Reviews*, 115, 37-75.
- Morley, C.K. & Arboit, F. 2019. Dating the onset of motion on the Sagaing fault: Evidence from detrital zircon and titanite U-Pb geochronology from the North Minwun Basin, Myanmar. *Geology*, 47, 581-585.
- Morley, C.K., Chantraprasert, S., Kongchum, J. & Chenoll, K. 2021. The West Burma Terrane, a review of recent paleo-latitude data, its geological implications and constraints. *Earth-Science Reviews*, 220, 103722.
- Müller, R.D., Cannon, J., Qin, X., Watson, R.J., Gurnis, M., Williams, S., Pfaffelmoser, T., Seton, M., Russell, S.H.J. & Zahirovic, S. 2018. GPlates: Building a Virtual Earth Through Deep Time. *Geochemistry, Geophysics, Geosystems*, 19, 2243-2261.
- Müller, R.D., Zahirovic, S., Williams, S.E., Cannon, J., Seton, M., Bower, D.J., Tetley, M., Heine, C., Le Breton, E., Liu, S., Russell, S.H.J., Yang, T., Leonard, J. & Gurnis, M. 2019. A global plate model including lithospheric deformation along major rifts and orogens since the Triassic. *Tectonics*, 38, 1884–1907.
- Najman, Y., Sobel, E.R., Millar, I., Stockli, D.F., Govin, G., Lisker, F., Garzanti, E., Limonta, M., Vezzoli, G., Copley, A., Zhang, P., Szymanski, E. & Kahn, A. 2020. The exhumation of the Indo-Burman Ranges, Myanmar. *Earth and Planetary Science Letters*, 530, 115948.
- Ng, S.W.-P., Whitehouse, M.J., Searle, M.P., Robb, L.J., Ghani, A.A., Chung, S.-L., Oliver, G.J.H., Sone, M., Gardiner, N.J. & Roselee, M.H. 2015. Petrogenesis of Malaysian granitoids in the Southeast Asian tin belt: Part 2. U-Pb zircon geochronology and tectonic model. *GSA Bulletin*, 127, 1238-1258.
- Obayashi, M., Yoshimitsu, J., Nolet, G., Fukao, Y., Shiobara, H., Sugioka, H., Miyamachi, H. & Gao, Y. 2013. Finite frequency whole mantle P wave tomography: Improvement of subducted slab images. *Geophysical Research Letters*, 40, 5652-5657.
- Österle, J.E., Klötzli, U., Stockli, D.F., Palzer-Khomenko, M. & Kanjanapayont, P. 2019. New age constraints on the Lan Sang gneiss complex, Thailand, and the timing of activity of the Mae Ping shear zone from in-situ and depth-profile zircon and monazite U-Th-Pb geochronology. *Journal of Asian Earth Sciences*, 181, 103886.
- Palin, R.M., Searle, M.P., Morley, C.K., Charusiri, P., Horstwood, M.S.A. & Roberts, N.M.W. 2013. Timing of metamorphism of the Lansang gneiss and implications for left-lateral motion along the Mae Ping (Wang Chao) strike-slip fault, Thailand. *Journal of Asian Earth Sciences*, 76, 120-136.
- Palin, R.M., Searle, M.P., St-Onge, M.R., Waters, D.J., Roberts, N.M.W., Horstwood, M.S.A., Parrish, R.R., Weller, O.M., Chen, S. & Yang, J. 2014. Monazite geochronology and petrology of

- kyanite- and sillimanite-grade migmatites from the northwestern flank of the eastern Himalayan syntaxis. *Gondwana Research*, 26, 323-347.
- Parsons, A.J., Hosseini, K., Palin, R. & Sigloch, K. 2020. Geological, geophysical and plate kinematic constraints for models of the India-Asia collision and the post-Triassic central Tethys oceans. *Earth-Science Reviews*, 103084.
- Patriat, P. & Achache, J. 1984. India–Eurasia collision chronology has implications for crustal shortening and driving mechanism of plates. *Nature*, 311, 615-621.
- Replumaz, A., Capitanio, F.A., Guillot, S., Negredo, A.M. & Villaseñor, A. 2014. The coupling of Indian subduction and Asian continental tectonics. *Gondwana Research*, 26, 608-626.
- Schaeffer, A.J. & Lebedev, S. 2013. Global shear speed structure of the upper mantle and transition zone. *Geophysical Journal International*, 194, 417-449.
- Schellart, W.P. 2005. Influence of the subducting plate velocity on the geometry of the slab and migration of the subduction hinge. *Earth and Planetary Science Letters*, 231, 197-219.
- Schellart, W.P., Stegman, D.R. & Freeman, J. 2008. Global trench migration velocities and slab migration induced upper mantle volume fluxes: Constraints to find an Earth reference frame based on minimizing viscous dissipation. *Earth-Science Reviews*, 88, 118-144.
- Searle, M.P., Noble, S.R., Cottle, J.M., Waters, D.J., Mitchell, A.H.G., Hlaing, T. & Horstwood, M.S.A. 2007. Tectonic evolution of the Mogok metamorphic belt, Burma (Myanmar) constrained by U-Th-Pb dating of metamorphic and magmatic rocks. *Tectonics*, 26.
- Searle, M.P., Elliott, J.R., Phillips, R.J. & Chung, S.L. 2011. Crustal–lithospheric structure and continental extrusion of Tibet. *Journal of the Geological Society*, 168, 633-672.
- Searle, M.P., Whitehouse, M.J., Robb, L.J., Ghani, A.A., Hutchison, C.S., Sone, M., Ng, S.W.-P., Roselee, M.H., Chung, S.-L. & Oliver, G.J.H. 2012. Tectonic evolution of the Sibumasu–Indochina terrane collision zone in Thailand and Malaysia: constraints from new U–Pb zircon chronology of SE Asian tin granitoids. *Journal of the Geological Society*, 169, 489-500.
- Searle, M.P., Morley, C.K., Waters, D.J., Gardiner, N.J., Kyi Htun, U., Nu, T.T. & Robb, L.J. 2017. Tectonic and metamorphic evolution of the Mogok Metamorphic and Jade Mines belts and ophiolitic terranes of Burma (Myanmar). In: Barber, A. J., Zaw, K. & Crow, M. J. (eds.) *Myanmar: Geology, Resources and Tectonics*. The Geological Society of London. 48, 261-293.
- Searle, M.P., Garber, J.M., Hacker, B.R., Htun, K., Gardiner, N.J., Waters, D.J. & Robb, L.J. 2020. Timing of Syenite-Charnockite Magmatism and Ruby and Sapphire Metamorphism in the Mogok Valley Region, Myanmar. *Tectonics*, 39, e2019TC005998.
- Seton, M., Müller, R.D., Zahirovic, S., Williams, S., Wright, N.M., Cannon, J., Whittaker, J.M., Matthews, K.J. & McGirr, R. 2020. A Global Data Set of Present-Day Oceanic Crustal Age and Seafloor Spreading Parameters. *Geochemistry, Geophysics, Geosystems*, 21, e2020GC009214.
- Sigloch, K. & Mihalynuk, M.G. 2017. Mantle and geological evidence for a Late Jurassic–Cretaceous suture spanning North America. *GSA Bulletin*, 129, 1489-1520.
- Simmons, N.A., Myers, S.C., Johannesson, G. & Matzel, E. 2012. LLNL-G3Dv3: Global P wave tomography model for improved regional and teleseismic travel time prediction. *Journal of Geophysical Research: Solid Earth*, 117.
- Simpson, A., Glorie, S., Morley, C.K., Roberts, N.M.W., Gillespie, J. & Lee, J.K. 2021. In-situ calcite U-Pb geochronology of hydrothermal veins in Thailand: New constraints on Indosinian and Cenozoic deformation. *Journal of Asian Earth Sciences*, 206, 104649.
- Sloan, R.A., Elliott, J.R., Searle, M.P., Morley, C.K., Barber, A.J., Zaw, K. & Crow, M.J. 2017. Active tectonics of Myanmar and the Andaman Sea. In: Barber, A. J., Zaw, K. & Crow, M. J. (eds.) *Myanmar: Geology, Resources and Tectonics*. The Geological Society of London. 48, 19-52.
- Smyth, H.R., Hall, R., Nichols, G.J., Draut, A.E., Clift, P.D. & Scholl, D.W. 2008. Cenozoic volcanic arc history of East Java, Indonesia: The stratigraphic record of eruptions on an active continental margin. In: Draut, A. E., Clift, P. D. & Scholl, D. W. (eds.) *Formation and Applications of the Sedimentary Record in Arc Collision Zones*. Geological Society of America. 436, 199-222.

- Spakman, W., Chertova, M.V., van den Berg, A. & van Hinsbergen, D.J.J. 2018. Puzzling features of western Mediterranean tectonics explained by slab dragging. *Nature Geoscience*, 11, 211-216.
- Steinberger, B., Torsvik, T.H. & Becker, T.W. 2012. Subduction to the lower mantle - a comparison between geodynamic and tomographic models. *Solid Earth*, 3, 415-432.
- Torsvik, T.H., Müller, R.D., Van der Voo, R., Steinberger, B. & Gaina, C. 2008. Global plate motion frames: Toward a unified model. *Reviews of Geophysics*, 46.
- Torsvik, T.H., Amundsen, H., Hartz, E.H., Corfu, F., Kuszniir, N., Gaina, C., Doubrovine, P.V., Steinberger, B., Ashwal, L.D. & Jamtveit, B. 2013. A Precambrian microcontinent in the Indian Ocean. *Nature Geoscience*, 6, 223-227.
- van de Lagemaat, S.H.A., van Hinsbergen, D.J.J., Boschman, L.M., Kamp, P.J.J. & Spakman, W. 2018. Southwest Pacific Absolute Plate Kinematic Reconstruction Reveals Major Cenozoic Tonga-Kermadec Slab Dragging. *Tectonics*, 37, 2647-2674.
- van der Meer, D.G., Spakman, W., van Hinsbergen, D.J.J., Amaru, M.L. & Torsvik, T.H. 2010. Towards absolute plate motions constrained by lower-mantle slab remnants. *Nature Geoscience*, 3, 36.
- van der Meer, D.G., van Hinsbergen, D.J.J. & Spakman, W. 2018. Atlas of the underworld: Slab remnants in the mantle, their sinking history, and a new outlook on lower mantle viscosity. *Tectonophysics*, 723, 309-448.
- van Hinsbergen, D.J.J., Lippert, P.C., Li, S., Huang, W., Advokaat, E.L. & Spakman, W. 2019. Reconstructing Greater India: Paleogeographic, kinematic, and geodynamic perspectives. *Tectonophysics*, 760, 69-94.
- Watkinson, I., Elders, C., Batt, G., Jourdan, F., Hall, R. & McNaughton, N.J. 2011. The timing of strike-slip shear along the Ranong and Khlong Marui faults, Thailand. *Journal of Geophysical Research: Solid Earth*, 116.
- Westerweel, J., Roperch, P., Licht, A., Dupont-Nivet, G., Win, Z., Poblete, F., Ruffet, G., Swe, H.H., Thi, M.K. & Aung, D.W. 2019. Burma Terrane part of the Trans-Tethyan arc during collision with India according to palaeomagnetic data. *Nature Geoscience*, 12, 863-868.
- Westerweel, J., Licht, A., Cogné, N., Roperch, P., Dupont-Nivet, G., Kay Thi, M., Swe, H.H., Huang, H., Win, Z. & Wa Aung, D. 2020. Burma Terrane Collision and Northward Indentation in the Eastern Himalayas Recorded in the Eocene-Miocene Chindwin Basin (Myanmar). *Tectonics*, 39, e2020TC006413.
- White, L.T., Hall, R., Armstrong, R.A., Barber, A.J., BouDagher Fadel, M., Baxter, A., Wakita, K., Manning, C. & Soesilo, J. 2017. The geological history of the Latimojong region of western Sulawesi, Indonesia. *Journal of Asian Earth Sciences*, 138, 72-91.
- Wu, J., Suppe, J., Lu, R. & Kanda, R. 2016. Philippine Sea and East Asian plate tectonics since 52 Ma constrained by new subducted slab reconstruction methods. *Journal of Geophysical Research: Solid Earth*, 121, 4670-4741.
- Zhang, X., Tien, C.-Y., Chung, S.-L., Maulana, A., Mawaleda, M., Chu, M.-F. & Lee, H.-Y. 2020. A Late Miocene magmatic flare-up in West Sulawesi triggered by Banda slab rollback. *GSA Bulletin*, 132, 2517-2528.
- Zhang, Z., Dong, X., Xiang, H., Ding, H., He, Z. & Liou, J.G. 2015. Reworking of the Gangdese magmatic arc, southeastern Tibet: post-collisional metamorphism and anatexis. *Journal of Metamorphic Geology*, 33, 1-21.
- Zhang, Z.M., Zhao, G.C., Santosh, M., Wang, J.L., Dong, X. & Liou, J.G. 2010. Two stages of granulite facies metamorphism in the eastern Himalayan syntaxis, south Tibet: petrology, zircon geochronology and implications for the subduction of Neo-Tethys and the Indian continent beneath Asia. *Journal of Metamorphic Geology*, 28, 719-733.
- Zhu, D.-C., Wang, Q., Chung, S.-L., Cawood, P.A. & Zhao, Z.-D. 2018. Gangdese magmatism in southern Tibet and India-Asia convergence since 120 Ma. *Geological Society, London, Special Publications*, 483, SP483.14.

627

628 **Figure 1.** Tectonic map of the Indian Ocean, showing outlines of Anomalies II, III and VII, and Late
629 Cretaceous-Cenozoic subduction magmatism. Plate boundaries, slab-depth profile, and seafloor
630 isochrons drawn from Bird (2003), Hayes et al. (2018) and Müller et al. (2019).

631 **Figure 2.** Select seismic tomography depth slices (a-c) and cross sections (d-f) with outlines of
632 seismic anomalies from P-wave tomography model UU-P07 (Amaru, 2007). (g-i) Outlines of
633 anomalies used for slab restorations (Figs. 3-4), are based on interpretation of six tomography
634 models and Slab2.0 model (see Supporting Information and Supporting Dataset).

635 **Figure 3.** (a-b) Reconstruction of two-stage India-Asia collision modified from Müller et al. (2019),
636 including Anomaly VII slab restoration. (c) Plate kinematics (Torsvik et al., 2008, Doubrovine et al.,
637 2012, Müller et al., 2019) highlighting plate network reorganisation events following Second
638 Collision at 45-40 Ma.

639 **Figure 4.** Cartoon representations of slab kinematics since Second Collision (45-40 Ma), looking
640 southwest. Anomaly VII divides into Indian (green) and Australian (purple) slabs, either side of the
641 extinct Wharton ridge. Coloured arrows show approximate slab motions. LSM of Anomaly II (blue)
642 occurs between (a) Second Collision and (b) slab break-off. Indian plate Anomaly VII slab (green) is
643 overturned and fragmented during northeast migration of India-Eurasia collision zone.

644

645

646

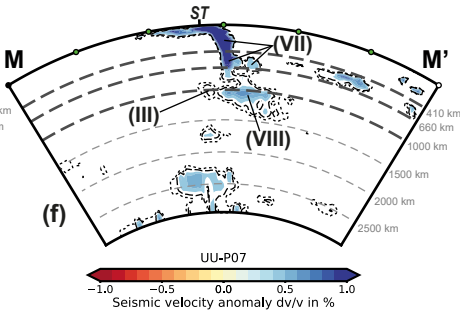
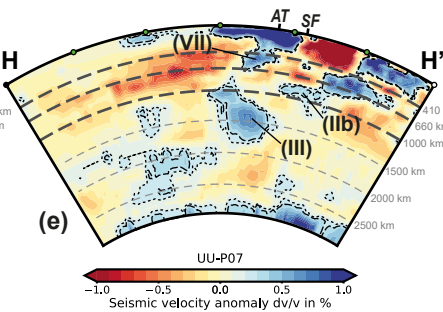
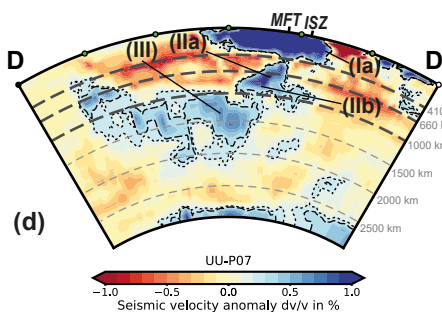
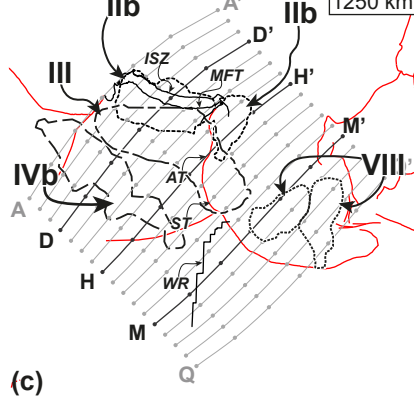
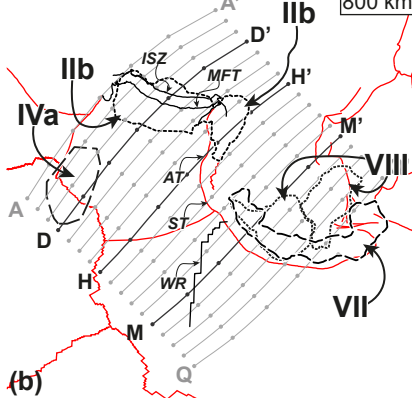
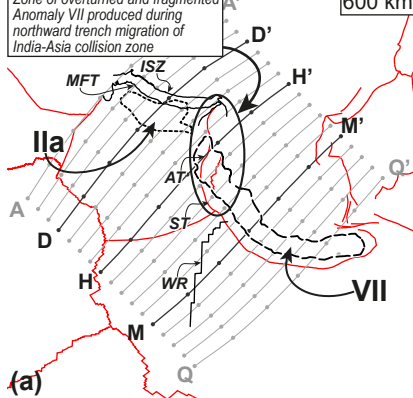


Zone of overturned and fragmented
Anomaly VII produced during
northward trench migration of
India-Asia collision zone

600 km

800 km

1250 km

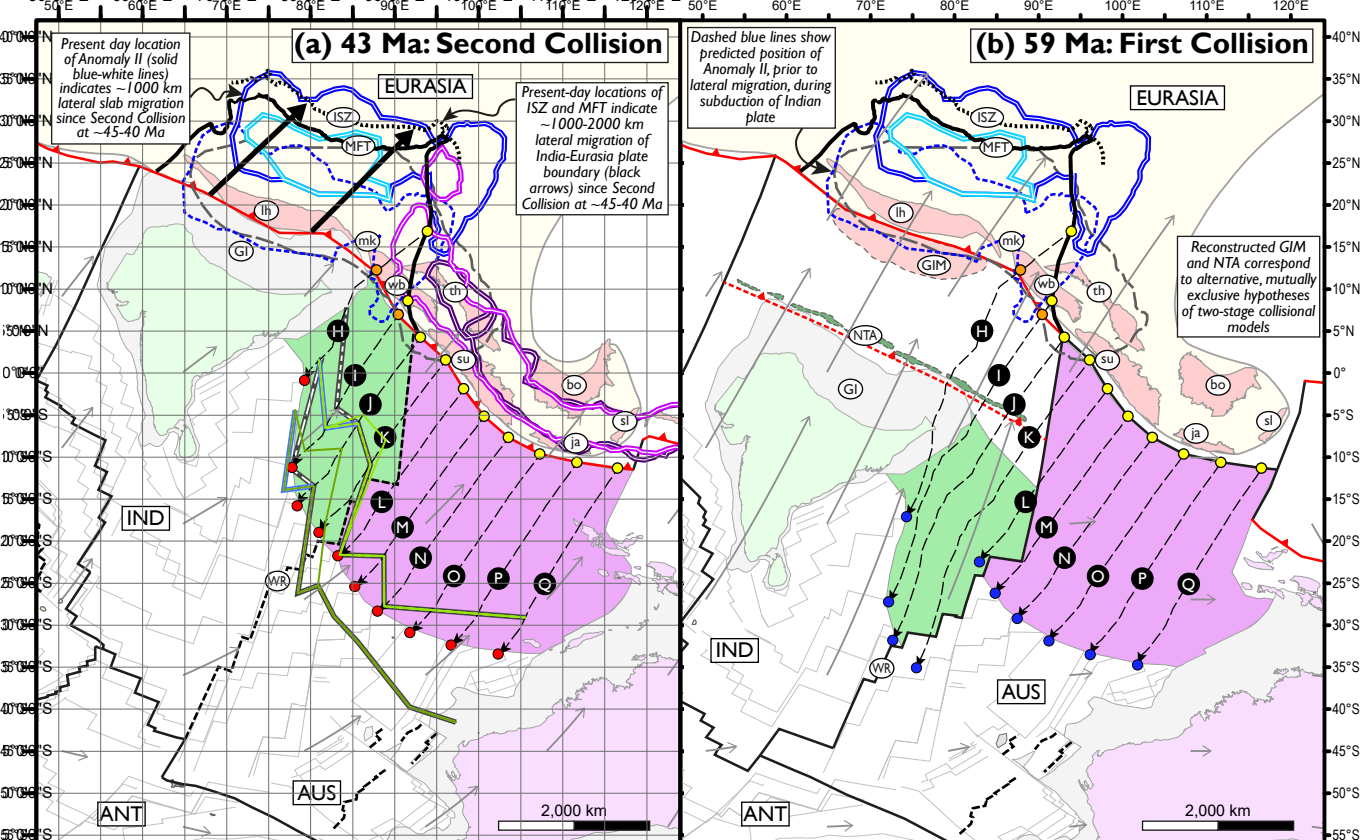


— Slab2.0 - slab outline

— +0.2% Anomaly Outline

--- +0.3% Anomaly Outline

NOTE: Anomaly VII is divided into Indian plate (VII-Ind) and Australian plate (VII-Aus)

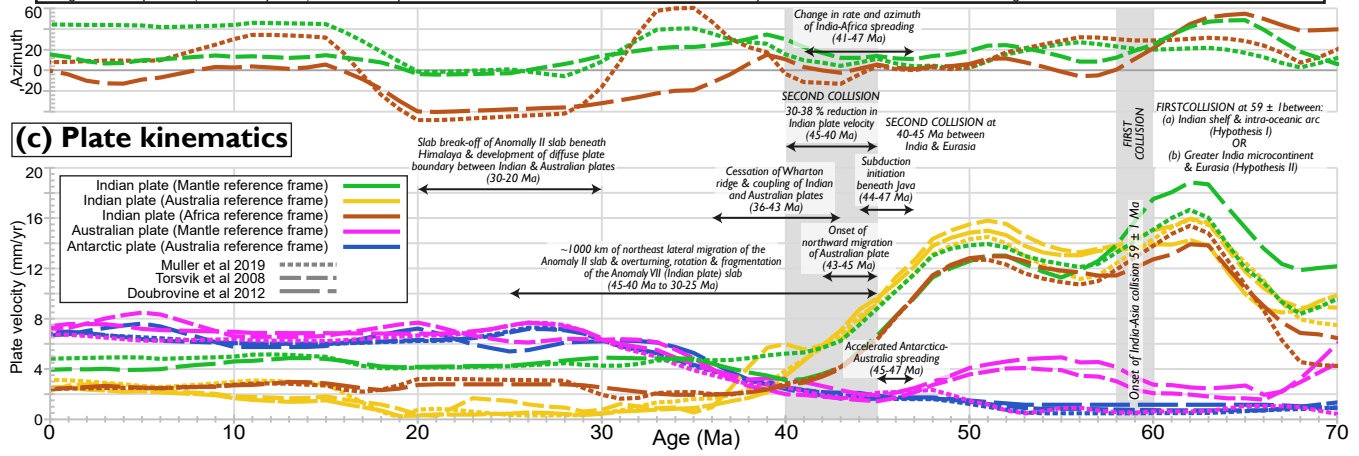


- Subduction plate boundary
- Spreading ridge / Transform plate boundary
- Extinct spreading ridge
- Fracture zone
- Seafloor isochron
- Plate velocity (relative to fixed mantle)
- Trench location at 0 Ma
- Restored trench location at 59-43 Ma
- Subduction boundary - two-stage collision Hypothesis I only

- Anomaly VII (~300 km to 600-700 km depth)
 - Anomaly VII (600-700 km to ~1000 km depth)
 - Anomaly II (450-550 km to 700-800 km depth)
 - Anomaly II (700-800 km to 1000-1300 km depth)
 - Anomaly II location prior to lateral migration (predicted)
 - Anomaly III (800-900 km to 1600-1700 km depth)
- NOTE: Anomaly VII at 0-300 km depth is omitted for clarity

- Restored Anomaly VII-Aus slab (Australian plate, subducted since ~43 Ma)
 - Restored Anomaly VII-Ind slab (Indian plate, subducted since ~43 Ma)
 - Maximum restored length of Anomaly VII slab, based on cross-section restoration
 - Minimum restored length of Anomaly VII slab, based on cross-section restoration
 - Maximum restored length of Anomaly VII slab + trench migration
 - Minimum restored length of Anomaly VII slab + trench migration
 - Top of restored Anomaly VII slab at 43 Ma, based on plate motions
 - Top of restored Anomaly VII slab at 59 Ma, based on plate motions
 - Plate motion path (letters correspond to cross sections)
- NOTE: Cross-section based Anomaly VII restorations follow plate motion paths
- Continental shelf (India and Australia)
 - Eurasian continent (Paleo-Pacific margin is approximated)
 - Restored locations of present-day coastlines and continental blocks (approximated)
 - Present day location of India-Eurasia plate boundary
 - Present day location of ISZ
 - Approximated migration of India-Eurasia plate boundary since 43 Ma
 - Neotethys intra-oceanic arc (NTA) - two-stage collision Hypothesis I only
 - Greater India microcontinent (GIM) - two-stage collision Hypothesis II only

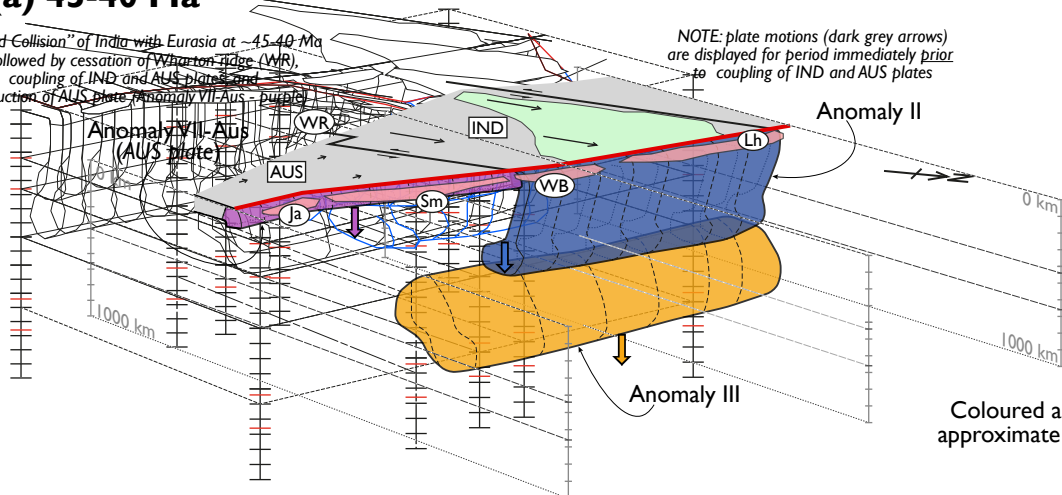
Abbreviations: ANT - Antarctic plate; AUS - Australian plate; bo - Borneo; GI - Greater India; GIM - Greater India microcontinent; IND - Indian plate; ISZ - Indus suture zone; ja - Java; lh - Lhasa block; MFT - Main frontal thrust; mk - Mogok metamorphic belt (northeast Myanmar); NTA - Neotethys intra-oceanic arc; sl - Sulawesi; su - Sumatra; th - Thailand-Malaysia; wb - West Burma block; WR - Wharton ridge



(a) 45-40 Ma

"Second Collision" of India with Eurasia at ~45-40 Ma is followed by cessation of Wharton ridge (WR), coupling of IND and AUS plates and subduction of AUS plate (Anomaly VII-Aus - purple)

NOTE: plate motions (dark grey arrows) are displayed for period immediately prior to coupling of IND and AUS plates



Coloured arrows show approximate slab motions

(b) 30-25 Ma

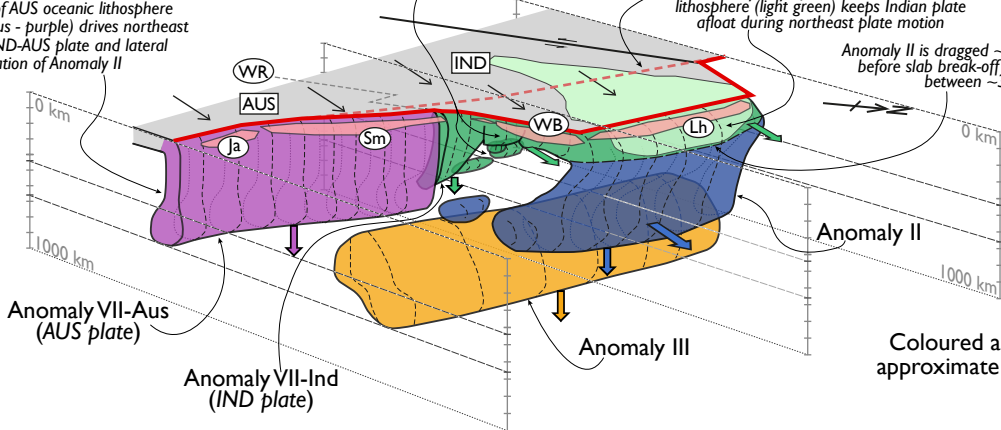
Lateral migration of India-Eurasia subduction zone results in overturning, fragmentation & clockwise rotation of subducting IND oceanic lithosphere (Anomaly VII-Ind - green) via 'unzipping' of Wharton ridge (WR) during subduction

Subduction of AUS oceanic lithosphere (Anomaly VII-Aus - purple) drives northeast motion of IND-AUS plate and lateral migration of Anomaly II

Location of Eurasian plate boundary at 43 Ma

Bouoyancy of IND continental lithosphere (light green) keeps Indian plate afloat during northeast plate motion

Anomaly II is dragged ~1,000 km northwards before slab break-off (thick dashed line) between ~30-25 Ma



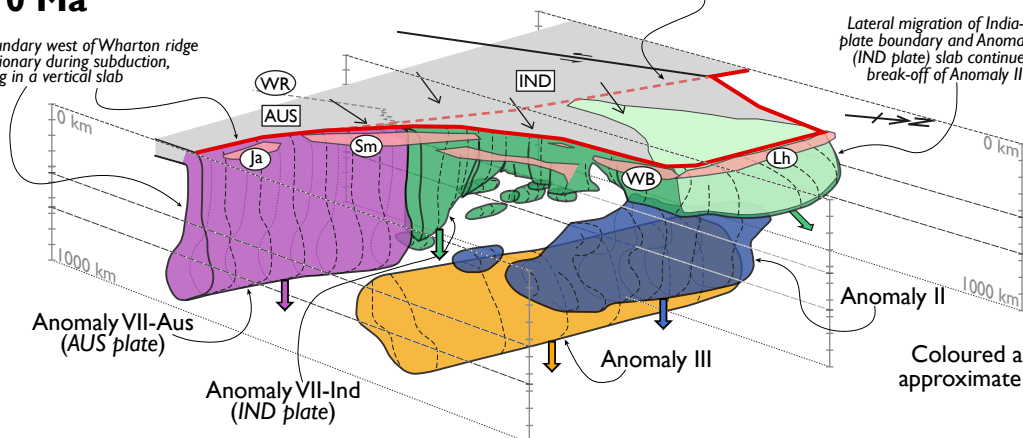
Coloured arrows show approximate slab motions

(c) 0 Ma

Eurasian plate boundary west of Wharton ridge remained stationary during subduction, resulting in a vertical slab

Location of Eurasian plate boundary at 43 Ma

Lateral migration of India-Eurasia plate boundary and Anomaly VII-Ind (IND plate) slab continues after break-off of Anomaly II slab



Coloured arrows show approximate slab motions

Abbreviations: AUS - Australian plate; IND - Indian plate; Ja - Java; Lh - Lhasa block; Sm - Sumatra; WB - West Burma block; WR - Wharton ridge